Linear and nonlinear light propagations in a Doppler-broadened medium via electromagnetically induced transparency

Liang Li
Department of Physics and Institute of Theoretical Physics, East China Normal University, Shanghai 200062, China

Guoxiang Huang*
State Key Laboratory of Precision Spectroscopy, East China Normal University, Shanghai 200062, China and Institute of Nonlinear Physics, Zhejiang Normal University, Zhejiang 321004, China

(Received 4 June 2010; published 18 August 2010)

We present a systematic theoretical study to deal with linear and nonlinear light propagations in a Doppler-broadened three-level Λ system via electromagnetically induced transparency (EIT), with incoherent population exchange between two lower energy levels taken into account. Through a careful analysis of base state and linear excitation, we show that the EIT condition of the system is given by $|\Omega_c|^2\gamma_{31} \gg 2\gamma_{21}\Delta\omega_D^2$, where Ω_c is half the Rabi frequency of the control field, $\Delta\omega_D$ is the Doppler width, and γ_{jl} is the decay rate of the coherence between states $|j\rangle$ and $|l\rangle$. Under this condition, the effect of incoherent population exchange is insignificant, while dephasing dominates the decoherence of the system. This condition also ensures the validity of the weak nonlinear perturbation theory used in this work for solving the Maxwell-Bloch equations with inhomogeneous broadening. We then investigate the nonlinear propagation of the probe field and show that it is possible to form temporal optical solitons in the Doppler-broadened medium. Such solitons have ultraslow propagating velocity and can be generated in very low light power. The possibility of realizing $(1+1)$-dimensional and $(2+1)$-dimensional spatial optical solitons in the adiabatic regime of the system is also discussed.

DOI: 10.1103/PhysRevA.82.023809 PACS number(s): 42.50.Gy, 42.65.Tg, 05.45.Yv

I. INTRODUCTION

Optics in coherent media has attracted tremendous attention due to the finding of electromagnetically induced transparency (EIT) and related quantum coherence phenomena [1–3]. It has been shown that EIT can be used not only for largely suppressing optical absorption, but also for substantially enhancing the efficiency of many nonlinear optical processes, including giant Kerr nonlinearity [4–15] four-wave mixing [16–28], optical solitons [29–37], and so on (see also Refs. [1–3] and cited references therein). Up to now, a large amount of theoretical work on linear and nonlinear properties of EIT systems has been carried out. However, in comparison with the study of cold atomic systems, EIT systems with inhomogeneous broadening have been less investigated, although many experiments have been made in hot atomic vapors in which the Doppler effect cannot be neglected. In addition, as far as we know, there is no report so far on nonlinear propagation of light pulses and beams and possible optical solitons in Doppler-broadened EIT systems.

There exist some previous theoretical studies on EIT-cored atomic systems with Doppler broadening, spanning the subjects of optimization of absorption reduction [38], narrowing of linewidth [39–48], effect of velocity-changing collisions [49,50], slowdown of light with both temporal and spatial dispersion effects [51], and so on [52–57]. In Ref. [38], a criterion for EIT for a Λ-type three-level system with Doppler broadening, i.e., $|\Omega_c|^2 \gg 2\sqrt{\ln 2}\gamma_{21}\Delta\omega_D$, was proposed, where Ω_c, $\Delta\omega_D$, and γ_{21} are half the Rabi frequency of the control field, the Doppler width, and the decay rate of the coherence between two lower levels $|2\rangle$ and $|1\rangle$, respectively. However, in another work [41], a different approach was given, in which an incoherent population exchange was introduced; this work stressed that one can still have EIT in the Doppler-broadened system if $|\Omega_c|^2 \gg \gamma_{21}\gamma_{31}$, which is nothing but the EIT criterion for a cold atomic system without inhomogeneous broadening. A recent experiment by Figueroa *et al.* [58] demonstrated that it is dephasing that plays a dominant role for the decoherence in the system, i.e., incoherent population exchange gives a negligible contribution to the width of the EIT transparency widow. In view of these different results, it is necessary to make a detailed investigation of pulse propagation and clarify the EIT condition in Doppler-broadened media.

In the present work, we make a systematic theoretical study of linear and nonlinear pulse propagation in a Doppler-broadened three-level Λ system. The aims of this work are twofold. First, we shall clarify the relative importance of decoherence mechanisms contributed by incoherent population exchange and dephasing, and propose a criterion for EIT in the three-level Λ system, i.e., $|\Omega_c|^2\gamma_{31} \gg 2\gamma_{21}\Delta\omega_D^2$. This criterion, valid for $\Delta\omega_D \gg \gamma_{31}$, is not only useful for clear appearance of EIT, but also ensures the validity of the self-consistent weak nonlinear perturbation method used in this work for solving the Maxwell-Bloch (MB) equations with inhomogeneous broadening. Second, we shall investigate the nonlinear propagation of a probe pulse and show that it is possible to form a temporal optical soliton in the Doppler-broadened Λ system under EIT conditions. This soliton has ultraslow propagating velocity and can be generated in very low light power. We shall also demonstrate both analytically and numerically the possibility of realizing $(1+1)$-dimensional [$(1+1)$D] and $(2+1)$D spatial optical solitons in the system.

*Corresponding author: gxhuang@phy.ecnu.edu.cn

The paper is arranged as follows. In the next section, we describe the model under study and discuss its linear property. A criterion for the appearance of EIT in a Λ-type three-level system with Doppler broadening is given. In Sec. III, we develop a weak nonlinear perturbation method for a density matrix with Doppler broadening and derive a nonlinear envelope equation for the probe pulse. We show that it is possible to realize an ultraslow optical soliton in the Doppler-broadened system. In Sec. IV, we demonstrate that the system can also support $(1+1)$D and $(2+1)$D spatial optical solitons. Finally, in Sec. V we give a discussion and summary of the main results obtained in this work.

II. THE MODEL AND ITS LINEAR PROPERTY

A. Model and base state solution

Consider an atomic system in which atoms have three energy levels with a Λ-type configuration, as shown in Fig. 1. The two lower states $|1\rangle$ and $|2\rangle$ are hyperfine ground states, while the state $|3\rangle$ is an excited state. A weak (strong) probe (control) field of central angular frequency ω_p (ω_c) couples to the atomic states $|1\rangle$ ($|2\rangle$) and $|3\rangle$. The quantities $\Delta_3=\omega_p-(\omega_3-\omega_1)$ and $\Delta_2=\omega_p-\omega_c-(\omega_2-\omega_1)$ are respectively one- and two-photon detunings for an atom at rest, with $\hbar\omega_j$ being the eigenenergy of the state $|j\rangle$ ($j=1,2,3$). Γ_{ij} represents the decay rate from state $|j\rangle$ to state $|i\rangle$. The electric-field vector of the system is $\mathbf{E}=\sum_{l=p,c}\mathbf{e}_l\mathcal{E}_l(z,t)e^{i(k_lz-\omega_lt)}+\text{c.c.}$, where $\mathbf{e}_l$ (k_l) is the unit polarization vector (wave number) of the electric-field component with the envelope $\mathcal{E}_l$ ($l=p,c$).

For a hot atomic vapor, the inhomogeneous broadening of the atomic radiation spectrum line due to the Doppler effect plays an important role in the optical response of the system. To include this effect, the external motion of the atoms must be taken into account properly. The interaction Hamiltonian of an atom and the optical field under the electric-dipole approximation and rotating-wave approximation is given by

$$\hat{\mathcal{H}}_I=-\hbar(\Omega_p^*e^{-i[k_p(z+vt)-\omega_pt]}|1\rangle\langle 3| + \Omega_c^*e^{-i[k_c(z+vt)-\omega_ct]}|2\rangle\langle 3|)+\text{H.c.}, \tag{1}$$

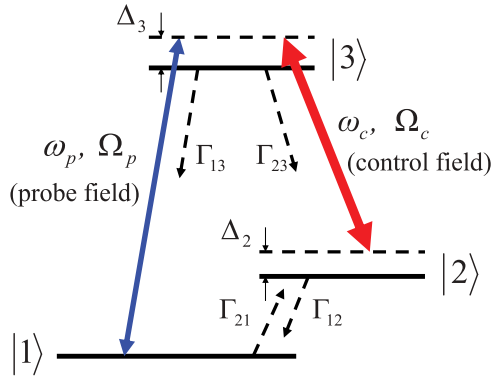

FIG. 1. (Color online) Energy-level diagram and excitation scheme of the three-level Λ system under study, in which a weak (strong) probe (control) field of central angular frequency ω_p (ω_c) and half Rabi frequency Ω_p (Ω_c) couples to the atomic states $|1\rangle$ ($|2\rangle$) and $|3\rangle$. Γ_{ij} denotes the incoherent decay rate from state $|j\rangle$ to state $|i\rangle$. Δ_2 and Δ_3 are two- and one-photon detunings for an atom at rest, respectively.

where $\Omega_{p(c)}=(\mathbf{e}_{p(c)}\cdot\mathbf{p}_{31(32)})\mathcal{E}_{p(c)}/\hbar$ is half the Rabi frequency of the probe (control) field, with $\mathbf{p}_{ij}$ being the electric-dipole matrix element associated with the transition from state $|j\rangle$ to state $|i\rangle$. When obtaining the above expression, we have assumed that the wave vectors of the probe and control fields are along the z direction, and the velocity of the atom is $\mathbf{v}$ with its z component being v. In the interaction picture, the density matrix elements are $\sigma_{ij}(\mathbf{r},v,t)=\rho_{ij}(\mathbf{r},v,t)\exp\{i[(k_j-k_i)(z+vt)-[(\omega_j-\omega_i)-(\Delta_j-\Delta_i)]t]\}$ $(i,j=1,2,3)$, with $k_1=0$, $k_2=k_p-k_c$, $k_3=k_p$, $\Delta_1=0$, and $\rho_{ij}(\mathbf{r},v,t)$ being the density matrix elements in the Schrödinger picture. The optical Bloch equations are given by

$$i\frac{\partial}{\partial t}\sigma_{11}+i\Gamma_{21}\sigma_{11}-i\Gamma_{12}\sigma_{22}-i\Gamma_{13}\sigma_{33}+\Omega_p^*\sigma_{31}-\Omega_p\sigma_{31}^*=0, \tag{2a}$$

$$i\frac{\partial}{\partial t}\sigma_{22}-i\Gamma_{21}\sigma_{11}+i\Gamma_{12}\sigma_{22}-i\Gamma_{23}\sigma_{33}+\Omega_c^*\sigma_{32}-\Omega_c\sigma_{32}^*=0, \tag{2b}$$

$$i\frac{\partial}{\partial t}\sigma_{33}+i\Gamma_3\sigma_{33}-\Omega_p^*\sigma_{31}+\Omega_p\sigma_{31}^*-\Omega_c^*\sigma_{32}+\Omega_c\sigma_{32}^*=0, \tag{2c}$$

$$\left(i\frac{\partial}{\partial t}+d_{21}\right)\sigma_{21}-\Omega_p\sigma_{32}^*+\Omega_c^*\sigma_{31}=0, \tag{2d}$$

$$\left(i\frac{\partial}{\partial t}+d_{31}\right)\sigma_{31}-\Omega_p(\sigma_{33}-\sigma_{11})+\Omega_c\sigma_{21}=0, \tag{2e}$$

$$\left(i\frac{\partial}{\partial t}+d_{32}\right)\sigma_{32}-\Omega_c(\sigma_{33}-\sigma_{22})+\Omega_p\sigma_{21}^*=0, \tag{2f}$$

where we have defined $d_{21}=-(k_p-k_c)v+\Delta_2+i\gamma_{21}$, $d_{31}=-k_pv+\Delta_3+i\gamma_{31}$, and $d_{32}=-k_cv+(\Delta_3-\Delta_2)+i\gamma_{32}$. The population and coherence decay rates are defined by $\Gamma_1=\Gamma_{21}$, $\Gamma_2=\Gamma_{12}$, $\Gamma_3=\Gamma_{13}+\Gamma_{23}$, and $\gamma_{ij}=\frac{1}{2}(\Gamma_i+\Gamma_j)+\gamma_{ij}^{\text{col}}$, respectively. Here γ_{ij}^{col} denotes the dipole dephasing rate caused by collisions. Notice that an incoherent population exchange from state $|1\rangle$ to state $|2\rangle$ is allowed in the model and hence one has nonvanishing Γ_{21}, which is the key factor to get the base state (7) given below. In addition, this is different from the model used in Ref. [41], where $\Gamma_{21}=\Gamma_{12}$ is assumed. In our model Γ_{21} and Γ_{12} are two independent parameters.

The propagation of electromagnetic waves is described by the Maxwell equation

$$\nabla^2\mathbf{E}-\frac{1}{c^2}\frac{\partial^2\mathbf{E}}{\partial t^2}=\frac{1}{\varepsilon_0c^2}\frac{\partial^2\mathbf{P}}{\partial t^2}. \tag{3}$$

Due to the Doppler effect, the electric polarization intensity of the system is given by

$$\mathbf{P}(\mathbf{r},t)=\mathcal{N}_a\int_{-\infty}^{\infty}dvf(v)[\mathbf{p}_{13}\sigma_{31}(\mathbf{r},v,t)e^{i(k_pz-\omega_pt)}+\mathbf{p}_{23}\sigma_{32}(\mathbf{r},v,t)e^{i(k_cz-\omega_ct)}+\text{c.c.}], \tag{4}$$

where $\mathcal{N}_a$ is the atomic concentration and $f(v)$ is the atomic velocity distribution profile. In thermal equilibrium, the velocity distribution profile is Maxwellian, i.e., $f(v)=1/(\sqrt{\pi}v_T)\exp[-(v/v_T)^2]$, with $v_T=(2k_BT/M)^{1/2}$ being the most probable atomic speed at temperature T. However, the integration over the Maxwellian distribution leads to a particular combination of error functions and is not easy

to analyze. Instead of using the Maxwellian distribution, a modified Lorentzian velocity distribution profile

$$f(v) = \frac{v_T/\sqrt{\pi}}{v_T^2 + v^2} \tag{5}$$

with the same Doppler width $\Delta\omega_D = k_p v_T$ is usually adopted to derive analytic expressions without losing the validity of the analysis [59].

Under the slow-varying-envelope approximation, Eq. (3) is reduced to the following form:

$$i\left(\frac{\partial}{\partial z} + \frac{1}{c}\frac{\partial}{\partial t}\right)\Omega_p + \frac{c}{2\omega_p}\left(\frac{\partial^2}{\partial x^2} + \frac{\partial^2}{\partial y^2}\right)\Omega_p + \kappa_{13}\int_{-\infty}^{\infty} dv f(v)\sigma_{31}(\mathbf{r}, v, t) = 0, \tag{6}$$

with $\kappa_{13} = \mathcal{N}_a\omega_p|\mathbf{p_{13}}|^2/(2\varepsilon_0 c\hbar)$. In deriving the above equation we have assumed that the Rabi frequency of the control field is strong enough so that Ω_c can be taken as a constant during time evolution.

The MB equations (2) and (6) provide us a framework to study the optical property of a system with the Doppler effect, which, by taking $v = 0$ in Eq. (2) and $f(v) = \delta(v)$ in Eq. (6), return to the equations of the corresponding cold atomic system. We choose a scheme in which the probe and control beams are copropagating along the z axis in order to maximally avoid the Doppler broadening of the two-photon transition, which is important to realize better EIT in the system.

The base state [60] of the system is that when the control field is applied but with the probe field absent. From MB Eqs. (2) and (6), it is easy to obtain the base state solution of the system,

$$\sigma_{11}^{(0)} = \frac{X_1\Gamma_{12}\Gamma_3 + \Gamma_{12}|\Omega_c|^2 + \Gamma_{13}|\Omega_c|^2}{X_2}, \tag{7a}$$

$$\sigma_{22}^{(0)} = \frac{X_1\Gamma_{21}\Gamma_3 + \Gamma_{21}|\Omega_c|^2}{X_2}, \tag{7b}$$

$$\sigma_{33}^{(0)} = \frac{\Gamma_{21}|\Omega_c|^2}{X_2}, \tag{7c}$$

$$\sigma_{32}^{(0)} = -\frac{\Omega_c}{d_{32}}\frac{X_1\Gamma_{21}\Gamma_3}{X_2}, \tag{7d}$$

$$\sigma_{21}^{(0)} = \sigma_{31}^{(0)} = 0, \tag{7e}$$

where we have defined $X_1 = \{[(\Delta_3 - \Delta_2) - k_c v]^2 + \gamma_{32}^2\}/(2\gamma_{32})$ and $X_2 = X_1(\Gamma_{21} + \Gamma_{12})\Gamma_3 + (2\Gamma_{21} + \Gamma_{12})|\Omega_c|^2 + \Gamma_{13}|\Omega_c|^2$.

It is helpful to make some remarks on the properties of the base state solution (7) and its implication for light propagation in the system. First, if $\Gamma_{21} = 0$, i.e., there is no incoherent population exchange, the ground state reduces to $\sigma_{11}^{(0)} = (X_1\Gamma_{12}\Gamma_3 + \Gamma_{12}|\Omega_c|^2 + \Gamma_{13}|\Omega_c^2)/X_2$, and $\sigma_{jl}^{(0)} = 0$ for $j \neq 1$ and $l \neq 1$, with X_1 unchanged but $X_2 = X_1\Gamma_{12}\Gamma_3 + \Gamma_{12}|\Omega_c|^2 + \Gamma_{13}|\Omega_c|^2$. That is to say, only state $|1\rangle$ is populated. This case has been discussed in Ref. [38]. Second, for nonvanishing Γ_{21}, state $|2\rangle$ and state $|3\rangle$ get populated. The magnitude of the population in different states is controlled by Γ_{21} and Ω_c. If the pumping effect by the control field dominates, the system is a well resonant one and all particles populate the state $|1\rangle$; in the opposite case, both the lower states $|1\rangle$ and $|2\rangle$ get populated. To illustrate these results quantitatively, we assume $k_p \simeq k_c$, and take $\Gamma_{13} \simeq \Gamma_{23} \simeq \gamma_{31} \simeq \gamma_{32}$ and $\gamma_{31} \gg \gamma_{21}, \Gamma_{12}, \Gamma_{21}$. Then we have (i) With a resonant control field (i.e., $\Delta_3 = \Delta_2$) and for a group of stationary atoms (i.e., $v = 0$), one has $\sigma_{11}^{(0)} \simeq 1$ and $\sigma_{22}^{(0)} \simeq 0$ if the condition

$$|\Omega_c|^2 \gg \gamma_{21}\gamma_{31} \tag{8}$$

is satisfied. Inequality (8) is nothing but the EIT condition obtained for cold atomic systems. (ii) For a group of atoms moving with speed around the most probable atomic speeds $\pm v_T$, only when the condition (8) and another condition

$$|\Omega_c|^2\gamma_{31} \gg 2\gamma_{21}\Delta\omega_D^2 \tag{9}$$

are satisfied simultaneously, can one obtain $\sigma_{11}^{(0)} \simeq 1$; hence we can say that the pumping effect by the control field dominates. At the other extreme, i.e., $|\Omega_c|^2\gamma_{31} \ll 2\gamma_{21}\Delta\omega_D^2$, the incoherent population exchange dominates, and hence one has $\sigma_{11}^{(0)} \simeq 1 - \Gamma_{21}/(2\gamma_{21})$ and $\sigma_{22}^{(0)} \simeq \Gamma_{21}/(2\gamma_{21})$. Consequently, when keeping the condition (8), by which the atomic group of nearly zero speed undergoes EIT, and at the same time keeping the condition (9), by which the atomic group of speed around $\pm v_T$ is strongly coupled with the optical field, one can say that the incoherent population exchange plays a negligible role in the base state. Because usually one has $\Delta\omega_D \gg \gamma_{31}$, the condition of negligible incoherent population exchange effect is thus given by Eq. (9), which is just the EIT condition in the present Doppler-broadened system, as will be shown below.

B. Linear dispersion relation

To obtain the EIT condition clearly, it is better to study the linear excitation of the system, which can be done by linearizing the MB equations (2) and (6). For simplicity, we assume that the system is homogeneous in the x and y directions. With this in mind, it is easy to get the linear dispersion relation of the system through taking $\sigma_{jj} = \sigma_{jj}^{(0)}$ $(j = 1,2,3)$, $\sigma_{32} = \sigma_{32}^{(0)}$ [given by Eq. (7)], Ω_p and σ_{j1} $(j = 2,3)$ being small quantities and proportional to $\exp(i\theta)$ with $\theta = K(\omega)z - \omega t$. Then we obtain the linear dispersion relation

$$K(\omega) = \frac{\omega}{c} + \kappa_{13}\int_{-\infty}^{\infty} dv f(v) \times \frac{(\omega + d_{21})\left(2\sigma_{11}^{(0)} + \sigma_{22}^{(0)} - 1\right) + \Omega_c\sigma_{32}^{*(0)}}{|\Omega_c|^2 - (\omega + d_{21})(\omega + d_{31})}, \tag{10}$$

The second term on the right-hand side (RHS) of Eq. (10) can be calculated by consideration of a contour integration in the complex plane and use of the residue theorem. For simplicity we take $\Delta_2 = \Delta_3 = 0$. In this case, we find two poles in the lower half complex plane, which are $k_p v = -ik_p v_T$ and $-i\sqrt{\gamma_{31}|\Omega_c|^2/(2\gamma_{21})}$. We take the contour consisting of the lower half complex plane and the real axis and denote $K(\omega) = \omega/c + \mathcal{K}_1 + \mathcal{K}_2$, where $\mathcal{K}_1$ and $\mathcal{K}_2$ are respectively obtained from the residual of the two poles in the lower complex half plane. The explicit expressions of $\mathcal{K}_1$ and $\mathcal{K}_2$ are given in the appendix.

By Taylor-expanding $K(\omega)$ as $K(\omega) = K_0 + K_1\omega + (1/2)K_2\omega^2 + (1/6)K_3\omega^3 + \cdots$, one can obtain the dispersion coefficients $K_j = [\partial^j K(\omega)/\partial\omega^j]|_{\omega=0}$ ($j = 0,1,2,3,\ldots$). Expressions for these dispersion coefficients can be obtained analytically but are omitted here because they are lengthy. The first coefficient K_0 describes the phase shift (real part) and the absorption (imaginary part) per unit length; the real parts of $1/K_1$ and $1/K_2$ represent the group velocity v_g and group-velocity dispersion, respectively.

At the center frequency of the probe field (i.e., at $\omega = 0$), we obtain the absorption

$$\mathrm{Im}(K_0) = \frac{\sqrt{\pi}\kappa_{13}}{\gamma_{21}\Delta\omega_D}\left(\frac{\gamma_{21}}{1+x_1} - \frac{\Gamma_{21}}{1+x_1}\frac{1}{1+\sqrt{x}}\right), \qquad (11)$$

where

$$x \equiv \frac{|\Omega_c|^2\gamma_{31}}{2\gamma_{21}\Delta\omega_D^2}, \quad x_1 \equiv \frac{|\Omega_c|^2}{\gamma_{21}\Delta\omega_D}. \qquad (12)$$

From Eq. (11) we obtain the following conclusions.

(i) For the probe-field propagation, the dephasing (denoted by γ_{21}) contributes an absorption, while the incoherent population exchange (denoted by Γ_{21}) contributes a gain. Physically, the absorption comes from the $|1\rangle \to |3\rangle \to |2\rangle$ transition carried out by the atoms initially populating $|1\rangle$ due to the dephasing, while the gain comes from the $|2\rangle \to |3\rangle \to |1\rangle$ transition carried out by the atoms initially populating $|2\rangle$ due to the incoherent population exchange.

(ii) If $x \gg 1$, the second term on the RHS of Eq. (11), which is contributed by the incoherent population exchange, is not significant, the linear optical property of the system contributes mainly through the $|1\rangle \to |3\rangle \to |2\rangle$ transition, and hence $\mathrm{Im}(K_0)$ is proportional to the first term of the RHS of Eq. (11). Since usually $\Delta\omega_D \gg \gamma_{31}$, when $x \gg 1$ one has also $x_1 \gg 1$. So in this case almost all atoms of the system undergo EIT.

(iii) When $x \simeq 1$, one still has $x_1 \gg 1$. In this situation, the second term on the RHS of Eq. (11) takes effect, i.e., the incoherent population exchange cannot be neglected. The atoms that exhibit the $|1\rangle \to |3\rangle \to |2\rangle$ transition undergo EIT, while other atoms that exhibit the $|2\rangle \to |3\rangle \to |1\rangle$ transition undergo an active Raman gain process. Because the whole system does not undergo a "pure" EIT, $x_1 \gg 1$ (i.e., $|\Omega_c|^2 \gg \gamma_{21}\Delta\omega_D$) cannot be taken as an EIT criterion of the system.

(iv) When $x \ll 1$ and $x_1 \ll 1$, there exists a competition between the absorption (contributed by dephasing) and the gain (contributed by incoherent population exchange). In this situation, on the one hand, the atoms that exhibit the $|1\rangle \to |3\rangle \to |2\rangle$ transition do not undergo EIT and hence there is a large absorption for the probe field. On the other hand, the atoms that exhibit the $|2\rangle \to |3\rangle \to |1\rangle$ transition undergo a Raman gain process, which suppresses the absorption and thus induces a dip in the absorption profile of the probe field [see Fig. 2(a)]. We must stress that the appearance of this dip is due to the gain contributed by the incoherent population exchange (i.e., by nonvanishing Γ_{21}), and hence cannot be taken as a manifestation of EIT of the system.

Based on the above analysis, we conclude that Eq. (9) (i.e., $x \gg 1$) can be taken as the criterion for EIT in the system with Doppler broadening and with nonvanishing incoherent population exchange (i.e., $\Gamma_{21} \neq 0$). This criterion also ensures the validity of the weak nonlinear perturbation theory developed in the next section for solving the MB equations with inhomogeneous broadening (see Sec. III B below).

If starting from the MB equations (2) and (6) in the absence of incoherent population exchange (i.e., $\Gamma_{21} = 0$), one can easily show that the EIT criterion for a Λ-type three-level system will be given by $x_1 \gg 1$ (or $|\Omega_c|^2 \gg \gamma_{21}\Delta\omega_D$). This criterion was proposed by Gea-Banacloche *et al.* [38], where only the decoherence due to dephasing was considered. In addition, for a ladder-type three-level system, since states $|1\rangle$ and $|2\rangle$ are greatly separated from each other, incoherent population exchange is insignificant. For such a system the EIT criterion is also given by $|\Omega_c|^2 \gg \gamma_{21}\Delta\omega_D$.

Figure 2(a) shows the profile of $\mathrm{Im}(K_0)$ as a function of $|\Omega_c|$ with $\Gamma_{21} = 0$ (line 1), $\Gamma_{21} = 0.5\gamma_{21}$ (line 2), and $\Gamma_{21} = \gamma_{21}$ (line 3), respectively. We see that for very large $|\Omega_c|$ (i.e., $x \gg 1$), $\mathrm{Im}(K_0)$ is small and no obvious difference for different Γ_{21} can be found; while for moderate and small $|\Omega_c|$ the Raman gain effect caused by Γ_{21} can be observed clearly. In particular, when $x_1 \ll 1$, a dip in the absorption profile induced by nonvanishing Γ_{21} appears, which is shown in the inset of Fig. 2(a).

Shown in Fig. 2(b) is the linewidth of transmission Γ as a function of control-field intensity. In the case $x \ll 1$, which corresponds to the left-hand side of the figure (with

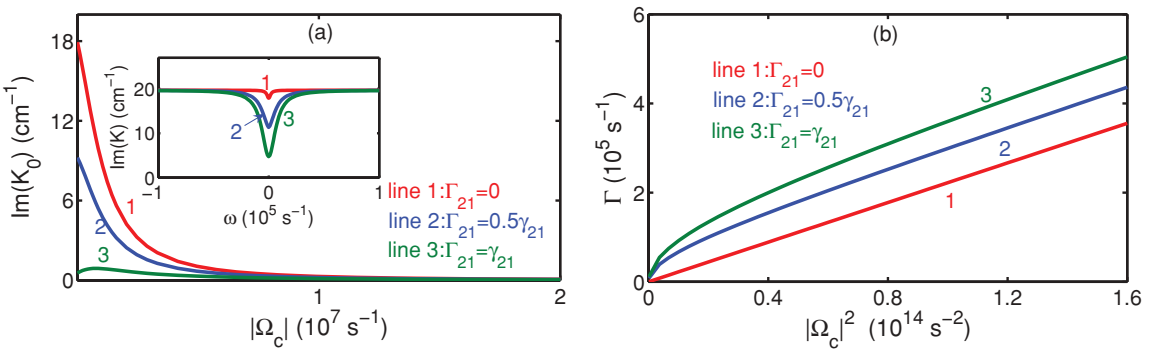

FIG. 2. (Color online) (a) $\mathrm{Im}(K_0)$ as a function of $|\Omega_c|$ for $2\Delta\omega_D = 100\gamma_{31}$ with different Γ_{21}. Inset shows the appearance of a small dip when Γ_{21} is increased for $x_1 = 0.1$. (b) Linewidth of transmission of the probe field as a function of control-field intensity for $2\Delta\omega_D = 100\gamma_{31}$ with different Γ_{21}. In both panels, lines 1, 2, and 3 are for $\Gamma_{21} = 0$, $\Gamma_{21} = 0.5\gamma_{21}$, and $\Gamma_{21} = \gamma_{21}$, respectively.

TABLE I. Comparison of linear optical properties, including absorption $\mathrm{Im}(K_0)$, group velocity v_g, and linewidth of transmission Γ, for several different regimes. Definitions of x and x_1 are given by Eq. (12). Other quantities have been defined in the text.

System	$\mathrm{Im}(K_0)$	v_g	Γ
Cold atom system	$\frac{\kappa_{13}\gamma_{21}}{\lvert\Omega_c\rvert^2}$	$(\frac{1}{c}+\frac{\kappa_{13}}{\lvert\Omega_c\rvert^2})^{-1}\simeq\frac{\lvert\Omega_c\rvert^2}{\kappa_{13}}$	$\frac{2\lvert\Omega_c\rvert^2}{\gamma_{31}}$
Hot atoms ($\Gamma_{21}\simeq\gamma_{21}, x\gg 1$)	$\sqrt{\pi}\frac{\kappa_{13}\gamma_{21}}{\lvert\Omega_c\rvert^2}$	$(\frac{1}{c}+\sqrt{\pi}\frac{\kappa_{13}}{\lvert\Omega_c\rvert^2})^{-1}\simeq\frac{\lvert\Omega_c\rvert^2}{\sqrt{\pi}\kappa_{13}}$	$\frac{2\lvert\Omega_c\rvert^2}{\Delta\omega_D}$
Hot atoms ($\Gamma_{21}\simeq\gamma_{21}, x\ll 1$)	$\sqrt{\pi}\frac{\kappa_{13}}{\Delta\omega_D}\sqrt{x}$	$(\frac{1}{c}+\sqrt{\pi}\frac{\kappa_{13}}{\lvert\Omega_c\rvert^2}\sqrt{x})^{-1}\simeq c$	$2\sqrt{\frac{2\gamma_{21}}{\gamma_{31}}}\lvert\Omega_c\rvert$
Hot atoms ($\Gamma_{21}=0, x_1\gg 1$)	$\sqrt{\pi}\frac{\kappa_{13}\gamma_{21}}{\lvert\Omega_c\rvert^2}$	$(\frac{1}{c}+\sqrt{\pi}\frac{\kappa_{13}}{\lvert\Omega_c\rvert^2})^{-1}\simeq\frac{\lvert\Omega_c\rvert^2}{\sqrt{\pi}\kappa_{13}}$	$\frac{2\lvert\Omega_c\rvert^2}{\Delta\omega_D}$
Hot atoms ($\Gamma_{21}=0, x_1\ll 1$)	$\sqrt{\pi}\frac{\kappa_{13}}{\Delta\omega_D}$	$(\frac{1}{c}+\sqrt{\pi}\frac{\kappa_{13}}{\gamma_{21}\Delta\omega_D})^{-1}\simeq\frac{\gamma_{21}\Delta\omega_D}{\sqrt{\pi}\kappa_{13}}$	0

$x=10^{-3}$ and $x_1=0.1$), a nonlinear dependence on $|\Omega_c|^2$ for very small $|\Omega_c|^2$ can be seen clearly for nonvanishing Γ_{21}. However, for large $|\Omega_c|^2$ the linewidth Γ becomes a linear function of $|\Omega_c|^2$ for any value of Γ_{21}, which corresponds to the right part of the figure (with $x=1$ and $x_1=100$). When plotting Fig. 2, we have used a practical example working with the D_1 line transition of ^{87}Rb atoms, in which $|5S_{1/2}, F=1\rangle$, $|5S_{1/2}, F=2\rangle$, and $|5P_{1/2}, F=1\rangle$ are selected as the atomic states $|1\rangle$, $|2\rangle$, and $|3\rangle$, respectively. The decay rates of coherence are assumed to have the relation $\gamma_{21}=10^{-4}\gamma_{31}$. Other parameters are taken as $\kappa_{13}=1.0\times10^{10}$ cm^{-1}s^{-1} and $2\Delta\omega_D=100\gamma_{31}$.

In Table I we have presented the calculated results for the linear optical properties of the system, including the absorption $\mathrm{Im}(K_0)$, group velocity v_g, and linewidth of transmission Γ, for several different regimes. In the calculation (and those in the rest of the paper), the condition (8) is assumed to be satisfied. The first line in Table I is for a cold atomic system. Values for $\mathrm{Im}(K_0)$, v_g, and Γ recover those obtained in previous studies [1–3]; the second and the third lines are for the Doppler-broadened system with $\Gamma_{21}\simeq\gamma_{21}$, which recover the result given in Ref. [41]; and the fourth line is for the Doppler-broadened system with $\Gamma_{21}=0$, which recovers the result of Ref. [38]. From the table we see that when EIT occurs, i.e., when $x\gg1$ or $x_1\gg1$, three systems (the first, second, and fourth lines in the table) have almost the same expressions for $\mathrm{Im}(K_0)$ and v_g (except for a factor π), but the Γ's are different. Interestingly, Γ in the Doppler-broadened systems can be obtained from that for the cold atomic system by replacing γ_{31} with $\Delta\omega_D$. In these three cases, the group velocity v_g becomes slow, and Γ has a linear dependence on the control-field intensity and hence possesses the feature of power broadening, which agrees well with the experimental result reported in Ref. [58]. The third (fifth) line of Table I is for a Doppler-broadened system with $\Gamma_{21}\simeq\gamma_{21}$ and $x\ll1$ ($\Gamma_{21}=0$ and $x_1\ll1$). No transparency happens because in this case Γ is very narrow (almost zero).

Shown in Fig. 3(a) is the absorption profile $\mathrm{Im}(K)$ as a function of ω when $2\Delta\omega_D=100\gamma_{31}$ and $\Gamma_{21}=\gamma_{21}$. Lines 1, 2, and 3 are for $\Omega_c=\gamma_{31}, 2\gamma_{31}$, and $3\gamma_{31}$, respectively. In this situation, the system works in the EIT regime (i.e., the effect due to the incoherent population change is suppressed). The width of the EIT transparency window is large, and it grows as $|\Omega_c|$ increases. Figure 3(b) shows the result for group-velocity dispersion, $\mathrm{Re}(K_2)$, for a given control field ($|\Omega_c|=2\gamma_{31}$) with different Doppler widths. Lines 1, 2, and 3 correspond to $2\Delta\omega_D=60\gamma_{31}$, $2\Delta\omega_D=80\gamma_{31}$, and $2\Delta\omega_D=100\gamma_{31}$, respectively. One can see that the group-velocity dispersion increases as the Doppler width $\Delta\omega_D$ increases.

At the linear level, for probe field with the Gaussian input form $\Omega_p(0,t)=\Omega_p(0,0)\exp(-t^2/\tau_0^2)$ we obtain its time evolution

$$\Omega_p(z,t)=\frac{\Omega_p(0,0)}{\sqrt{b_1(z)-ib_2(z)}}\exp\left(iK_0z-\frac{(K_1z-t)^2}{[b_1(z)-ib_2(z)]\tau_0^2}\right), \tag{13}$$

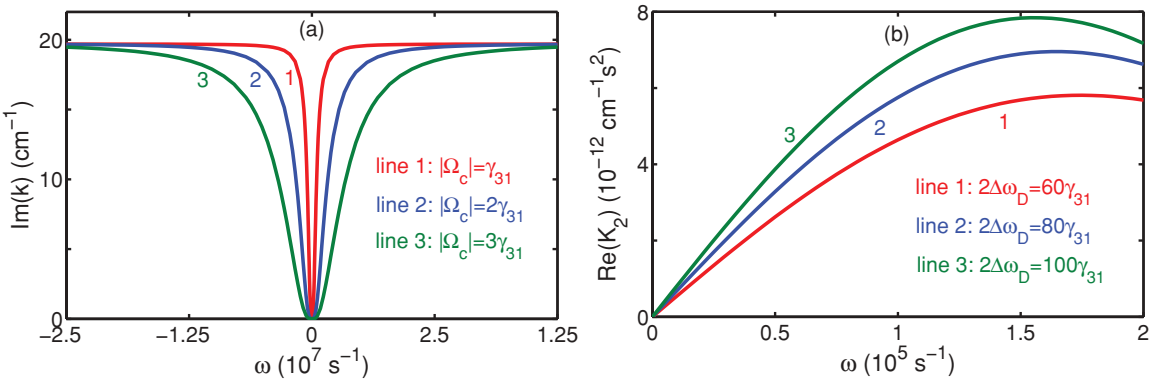

FIG. 3. (Color online) Absorption and group-velocity dispersion when the system is in the EIT regime. (a) $\mathrm{Im}(K)$ as a function of ω for $2\Delta\omega_D=100\gamma_{31}$. Lines 1, 2, and 3 are for $\Omega_c=\gamma_{31}, 2\gamma_{31}$, and $3\gamma_{31}$, respectively. (b) Group-velocity dispersion of the system for $|\Omega_c|=2\gamma_{31}$. From bottom to top, $2\Delta\omega_D=60\gamma_{31}$, $2\Delta\omega_D=80\gamma_{31}$, and $2\Delta\omega_D=100\gamma_{31}$, respectively.

where $b_1(z) = 1 + 2zK_{2i}/\tau_0^2, b_2(z) = 2zK_{2r}/\tau_0^2$ with $K_2 = K_{2r} + iK_{2i}$; $\Omega_p(0,0)$ and τ_0 are the initial half Rabi frequency of the probe pulse and the pulse duration, respectively. We see that, although the absorption can be greatly suppressed by the EIT effect [i.e., $\mathrm{Im}(K_j)$ $(j = 0,1,2)$ become small], the dispersion results in a rapid spreading of the probe pulse during propagation.

III. WEAK-LIGHT ULTRASLOW SOLITONS

One of our main interests is to obtain a shape-preserving propagation of the probe pulse, which is desirable for the application of optical information processing and transmission. Because the system under study is a highly resonant one, as shown above the linear propagation of the probe pulse displays a strong dispersion, which results in pulse distortion. To obtain a probe pulse that is robust during propagation, it is natural to increase the probe-field intensity to realize a balance between the dispersion and nonlinear effects of the system. One of such stable pulses is the optical soliton, which we shall explore in the following.

A. Kerr nonlinearity of the system

Before studying optical solitons, we make a simple discussion of Kerr nonlinearity of the system. From the MB equations (2) and (6), it is easy to get the probe-field susceptibility

$$\chi_p = \int_v dv f(v) \frac{\mathcal{N}_a |\mathbf{p_{13}}|^2}{\varepsilon_0 \hbar} \frac{\sigma_{31}}{\Omega_p} \approx \chi_p^{(1)} + \chi_{pp}^{(3)} |\mathcal{E}_p|^2 \tag{14}$$

with $\chi_p^{(1)}$ and $\chi_{pp}^{(3)}$ being the linear susceptibility and third-order (Kerr) susceptibility, respectively. Solving σ_{31} from Eqs. (2a)–(2f) under the steady-state approximation and making a Taylor expansion with respect to $|\Omega_p|$, we obtain

$$\chi_p^{(1)} = \frac{\mathcal{N}_a |\mathbf{P}_{13}|^2}{\varepsilon_0 \hbar} \int_v dv f(v) T_1, \tag{15a}$$

$$\chi_{pp}^{(3)} = \frac{\mathcal{N}_a |\mathbf{P}_{13}|^4}{\varepsilon_0 \hbar^3} \int_v dv f(v) \times \frac{iJ_1(T_1 - \text{c.c.}) + iJ_2(d_{32}\Omega_c T_2 - \text{c.c.}) + \Omega_c T_2}{d_{32}^*(|\Omega_c|^2 - d_{21}d_{31})}, \tag{15b}$$

with

$$T_1 = \frac{d_{21}[\gamma_{31}|\Omega_c|^2 + \gamma_{21}(k_p v)^2] + \gamma_{21}|\Omega_c|^2(k_p v - i\gamma_{31})}{[\gamma_{31}|\Omega_c|^2 + 2\gamma_{21}(k_p v)^2](|\Omega_c|^2 - d_{21}d_{31})}, \tag{16a}$$

$$T_2 = \frac{d_{31}\gamma_{21}\Omega_c^*(k_p v - i\gamma_{31}) + \Omega_c^*[\gamma_{31}|\Omega_c|^2 + \gamma_{21}(k_p v)^2]}{[\gamma_{31}|\Omega_c|^2 + 2\gamma_{21}(k_p v)^2](|\Omega_c|^2 - d_{21}d_{31})}, \tag{16b}$$

$$J_1 = (|\Omega_c|^2 + d_{21}d_{32}^*) \frac{4|\Omega_c|^2 + (k_p v)^2 + \gamma_{31}^2}{2\gamma_{31}|\Omega_c|^2 + 4\gamma_{21}(k_p v)^2} - \frac{2|\Omega_c|^2 - d_{21}d_{32}^*}{\gamma_{31}}, \tag{16c}$$

$$J_2 = \frac{|\Omega_c|^2 + d_{21}d_{32}^*}{2\gamma_{31}|\Omega_c|^2 + 4\gamma_{21}(k_p v)^2}. \tag{16d}$$

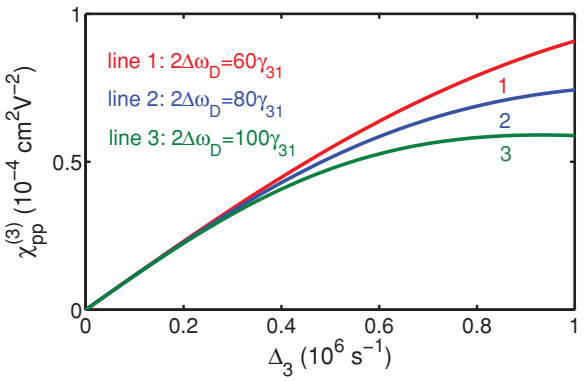

FIG. 4. (Color online) Third-order susceptibility $|\chi_{pp}^{(3)}|$ as a function of Δ_3. Lines 1, 2, and 3 are for Doppler width $2\Delta\omega_D = 60\gamma_{31}$, $2\Delta\omega_D = 80\gamma_{31}$, and $2\Delta\omega_D = 100\gamma_{31}$, respectively.

The use of the modified Lorentzian distribution (5) gives $\chi_p^{(1)} = 2(\mathcal{K}_1 + \mathcal{K}_2)/k_p$, with $\mathcal{K}_1$ and $\mathcal{K}_2$ the same as those given in Eqs. (A1) and (A3), but the variable ω being replaced by Δ_3. $\chi_{pp}^{(3)}$ can also be evaluated by use of the residue theorem. The result is quite lengthy and hence not listed explicitly here. Shown in Fig. 4 is the profile of $|\chi_{pp}^{(3)}|$ versus the detuning Δ_3 inside the EIT transparency window. Parameters are the same as those used in Fig. 3(b). We see that at the central point ($\Delta_3 = 0$), where the system undergoes an ideal EIT, no nonlinearity exists. Therefore, to obtain a nonlinear effect a deviation from the ideal EIT is necessary. This is the same as the case of cold atomic systems [29–37]. Indeed, $|\chi_{pp}^{(3)}|$ grows as Δ_3 increases. Shown in Fig. 4 is $|\chi_{pp}^{(3)}|$ as a function of Δ_3. Lines 1, 2, and 3 in the figure are for the Doppler width $2\Delta\omega_D = 60\gamma_{31}$, $2\Delta\omega_D = 80\gamma_{31}$, and $2\Delta\omega_D = 100\gamma_{31}$, respectively. We see that the Kerr nonlinearity is inversely proportional to the Doppler width, which means that, to obtain a large Kerr effect, the temperature of the system cannot be too high.

B. Asymptotic expansion and nonlinear envelope equation

We now begin to study the nonlinear pulse propagation in the system by using a weak nonlinear perturbation theory. Recently, a method of multiple scales for solving MB equations for cold atomic systems has been developed [61]. Here we extend this method to the present Doppler-broadened hot atomic system. We take the following asymptotic expansion:

$$\sigma_{jj} - \sigma_{jj}^{(0)} = \epsilon^2 \sigma_{jj}^{(2)} + \epsilon^3 \sigma_{jj}^{(3)} + \cdots (j = 1,2,3), \tag{17a}$$

$$\sigma_{j1} = \epsilon \sigma_{j1}^{(1)} + \epsilon^2 \sigma_{j1}^{(2)} + \epsilon^3 \sigma_{j1}^{(3)} + \cdots (j = 2,3), \tag{17b}$$

$$\sigma_{32} - \sigma_{32}^{(0)} = \epsilon^2 \sigma_{32}^{(2)} + \epsilon^3 \sigma_{32}^{(3)} + \cdots, \tag{17c}$$

$$\Omega_p = \epsilon \Omega_p^{(1)} + \epsilon^2 \Omega_p^{(2)} + \epsilon^3 \Omega_p^{(3)} + \cdots, \tag{17d}$$

where $\sigma_{ij}^{(0)}$ is the base state solution given by Eq. (7), and ϵ is a dimensionless small parameter characterizing the small depletion of the ground state $|1\rangle$. All quantities on the right-hand side of the expansion are considered as functions of the multiscale variables $z_n = \epsilon^n z$ $(n = 0,1,2)$, $t_n = \epsilon^n t$ $(n = 0,1)$, $x_1 = \epsilon x$, and $y_1 = \epsilon y$. Notice that to make the weak nonlinear theory valid, all quantities on the RHS of the above expansion that are proportional to $\epsilon^{(j)}$ $(j = 1,2,\ldots)$ must be

finite during pulse propagation. For the Doppler-broadened system, this requirement means that Ω_p cannot have large gain coming from the incoherent population exchange Γ_{21}. In other words, the system must work in the EIT condition given by the inequality (9).

Substituting the expansion (17) into the MB equations (2a)–(2f) and (6), we obtain a series of equations for $\sigma_{ij}^{(l)}$ and $\Omega_p^{(l)}$ $(l = 1,2,3)$:

$$i\left(\frac{\partial}{\partial z_0}+\frac{1}{c}\frac{\partial}{\partial t_0}\right)\Omega_p^{(l)}+\kappa_{13}\int_v dv f(v)\sigma_{31}^{(l)}=M^{(l)}, \quad (18a)$$

$$\left(i\frac{\partial}{\partial t_0}+d_{21}\right)\sigma_{21}^{(l)}-\Omega_p^{(l)}\sigma_{32}^{*(0)}+\Omega_c^*\sigma_{31}^{(l)}=N^{(l)}, \quad (18b)$$

$$\left(i\frac{\partial}{\partial t_0}+d_{31}\right)\sigma_{31}^{(l)}-\Omega_p^{(l)}\left(2\sigma_{11}^{(0)}+\sigma_{22}^{(0)}-1\right)+\Omega_c\sigma_{21}^{(l)}=P^{(l)}, \quad (18c)$$

$$\left(i\frac{\partial}{\partial t_0}+d_{32}\right)\sigma_{32}^{(l)}+\Omega_c\left(\sigma_{11}^{(l)}+2\sigma_{22}^{(l)}\right)=Q^{(l)}, \quad (18d)$$

$$i\frac{\partial}{\partial t_0}\sigma_{11}^{(l)}+i(\Gamma_{21}+\Gamma_{13})\sigma_{11}^{(l)}-i(\Gamma_{12}-\Gamma_{13})\sigma_{22}^{(l)}=Y^{(l)}, \quad (18e)$$

$$i\frac{\partial}{\partial t_0}\sigma_{22}^{(l)}+i(\Gamma_{12}+\Gamma_{23})\sigma_{22}^{(l)}-i(\Gamma_{21}-\Gamma_{23})\sigma_{11}^{(l)}+\Omega_c^*\sigma_{32}^{(l)}-\Omega_c\sigma_{32}^{*(l)}=Z^{(l)}, \quad (18f)$$

which can be solved order by order in a systematic way. The explicit expressions for $M^{(l)}$, $N^{(l)}$, $P^{(l)}$, $Q^{(l)}$, $Y^{(l)}$, and $Z^{(l)}$ $(l = 1,2,3)$ can be systematically and analytically derived; they are omitted to save space.

(i) *First-order approximation*. The leading order $l = 1$ is the linear excitation studied in Sec. II. The solution reads

$$\Omega_p^{(1)}=Fe^{i\theta}, \quad (19a)$$

$$\sigma_{31}^{(1)}=\frac{(\omega+d_{21})\left(2\sigma_{11}^{(0)}+\sigma_{22}^{(0)}-1\right)+\Omega_c\sigma_{32}^{(0)}}{|\Omega_c|^2-(\omega+d_{21})(\omega+d_{31})}Fe^{i\theta}, \quad (19b)$$

$$\sigma_{21}^{(1)}=-\frac{(\omega+d_{31})\sigma_{32}^{*(0)}+\Omega_c^*\left(2\sigma_{11}^{(0)}+\sigma_{22}^{(0)}-1\right)}{|\Omega_c|^2-(\omega+d_{21})(\omega+d_{31})}Fe^{i\theta}, \quad (19c)$$

where F is a yet-to-be determined envelope function depending on the slow variables z_1, z_2, and t_1; $\theta = Kz_0 - \omega t_0$ with K (linear dispersion relation) given by Eq. (10).

(ii) *Second-order approximation*. In the second order $(l = 2)$, a divergence-free solution for $\Omega_p^{(2)}$ requires

$$i\left(\frac{\partial F}{\partial z_1}+\frac{\partial K}{\partial\omega}\frac{\partial F}{\partial t_1}\right)=0, \quad (20)$$

which shows that the envelope function F travels with complex group velocity $(\partial K/\partial\omega)^{-1}$. The second-order solution reads

$$\Omega_p^{(2)}=0, \quad \sigma_{11}^{(2)}=a_{11}^{(2)}|F|^2e^{-2\tilde{\alpha}z_2}, \quad \sigma_{22}^{(2)}=a_{22}^{(2)}|F|^2e^{-2\tilde{\alpha}z_2}, \quad \sigma_{32}^{(2)}=a_{32}^{(2)}|F|^2e^{-2\tilde{\alpha}z_2}, \quad (21a)$$

$$\sigma_{31}^{(2)}=i\frac{[|\Omega_c|^2+(\omega+d_{21})^2]\left(2\sigma_{11}^{(0)}+\sigma_{22}^{(0)}-1\right)+(2\omega+d_{21}+d_{31})\Omega_c\sigma_{32}^{*(0)}}{[|\Omega_c|^2-(\omega+d_{21})(\omega+d_{31})]^2}\frac{\partial}{\partial t_1}Fe^{i\theta}, \quad (21b)$$

$$\sigma_{21}^{(2)}=i\frac{(2\omega+d_{21}+d_{31})\Omega_c^*\left(1-2\sigma_{11}^{(0)}-\sigma_{22}^{(0)}\right)-[|\Omega_c|^2+(\omega+d_{31})^2]\sigma_{32}^{*(0)}}{[|\Omega_c|^2-(\omega+d_{21})(\omega+d_{31})]^2}\frac{\partial}{\partial t_1}Fe^{i\theta}, \quad (21c)$$

with $\alpha = \mathrm{Im}(K) = \epsilon^2\tilde{\alpha}$. The explicit expressions of $a_{11}^{(2)}$, $a_{22}^{(2)}$, and $a_{32}^{(2)}$ are

$$a_{11}^{(2)}=\left\{\left[i(\Gamma_{12}+\Gamma_{23})+2|\Omega_c|^2\left(\frac{1}{d_{32}^*}-\frac{1}{d_{32}}\right)\right]\left(\frac{(\omega+d_{21}^*)\left(2\sigma_{11}^{(0)}+\sigma_{22}^{(0)}-1\right)+\Omega_c^*\sigma_{32}^{(0)}}{|\Omega_c|^2-(\omega+d_{21}^*)(\omega+d_{31}^*)}-\text{c.c.}\right)\right.$$
$$\left.-i(\Gamma_{13}-\Gamma_{12})\left(\frac{\Omega_c}{d_{32}^*}\frac{(\omega+d_{31})\sigma_{32}^{*(0)}+\Omega_c^*\left(2\sigma_{11}^{(0)}+\sigma_{22}^{(0)}-1\right)}{|\Omega_c|^2-(\omega+d_{21})(\omega+d_{31})}-\text{c.c.}\right)\right\}\Bigg/\left[i|\Omega_c|^2(2\Gamma_{21}+\Gamma_{12}+\Gamma_{13})\left(\frac{1}{d_{32}^*}-\frac{1}{d_{32}}\right)\right.$$
$$\left.-\Gamma_3(\Gamma_{12}+\Gamma_{21})\right], \quad (22a)$$

$$a_{22}^{(2)}=\frac{-i}{\Gamma_{13}-\Gamma_{12}}\left\{\left(\frac{(\omega+d_{21}^*)\left(2\sigma_{11}^{(0)}+\sigma_{22}^{(0)}-1\right)+\Omega_c^*\sigma_{32}^{(0)}}{|\Omega_c|^2-(\omega+d_{21})(\omega+d_{31})}-\text{c.c.}\right)-i(\Gamma_{21}+\Gamma_{13})a_{11}^{(2)}\right\}, \quad (22b)$$

$$a_{32}^{(2)}=\frac{1}{d_{32}}\left(\frac{(\omega+d_{31}^*)\sigma_{32}^{(0)}+\Omega_c\left(2\sigma_{11}^{(0)}+\sigma_{22}^{(0)}-1\right)}{|\Omega_c|^2-(\omega+d_{21}^*)(\omega+d_{31}^*)}-\Omega_c\left(a_{11}^{(2)}+2a_{22}^{(2)}\right)\right). \quad (22c)$$

(iii) *Third-order approximation*. This is the order ($l = 3$) in which the Kerr nonlinearity plays a role. A divergence-free solution for $\Omega_p^{(3)}$ requires

$$i\frac{\partial F}{\partial z_2} + \frac{c}{2\omega_p}\left(\frac{\partial^2}{\partial x_1^2} + \frac{\partial^2}{\partial y_1^2}\right)F - \frac{1}{2}\frac{\partial^2 K}{\partial \omega^2}\frac{\partial^2 F}{\partial t_1^2} - W|F|^2 F e^{-2\tilde{\alpha} z_2} = 0, \tag{23}$$

where

$$W = -\kappa_{13}\int_v dv f(v)\frac{\Omega_c a_{32}^{*(2)} + (\omega + d_{21})\left(2a_{11}^{(2)} + a_{22}^{(2)}\right)}{|\Omega_c|^2 - (\omega + d_{21})(\omega + d_{31})}. \tag{24}$$

Combination of Eqs. (20) and (23) gives the nonlinear envelope equation

$$i\left(\frac{\partial}{\partial z} + \alpha\right)U + \frac{c}{2\omega_p}\left(\frac{\partial^2}{\partial x_1^2} + \frac{\partial^2}{\partial y_1^2}\right)U - \frac{1}{2}\frac{\partial^2 K}{\partial \omega^2}\frac{\partial^2 U}{\partial \tau^2} - W|U|^2 U e^{-2\alpha z} = 0, \tag{25}$$

where $\tau = t - z/v_g$ and $U = \epsilon F \exp(-i\alpha z)$.

C. Ultraslow solitons at low light level

The formation and propagation of an optical soliton in the system requires the following conditions. First, there is a balance between the dispersion and nonlinearity. Second, the absorption of the probe field is negligibly small. In general, coefficients of the envelope Eq. (25) are complex, which means that a soliton solution, even if it exists and is produced, may be highly unstable during propagation. However, if a realistic set of system parameters under some condition can be found so that the imaginary part of these coefficients can be much smaller than their corresponding real part, it is possible to get a shape-preserving, localized solution that can propagate a rather long distance without a significant distortion. In the present system, the condition of relatively small imaginary parts of the coefficients is nothing but the EIT condition (9). Under this condition, Eq. (25) with neglect of the small imaginary part of the coefficients can be written in the dimensionless form

$$i\frac{\partial u}{\partial s} + \frac{\partial^2 u}{\partial \sigma^2} + 2|u|^2 u = id_0 u + d_1\left(\frac{\partial^2}{\partial \xi_1^2} + \frac{\partial^2}{\partial \eta_1^2}\right)u, \tag{26}$$

where $s = -z/(2L_D)$, $\sigma = \tau/\tau_0$, $(\xi,\eta) = (x,y)/R_\perp$, and $u = U/U_0$. $L_D = \tau_0^2/K_{2r}$ is the characteristic dispersion length, $R_\perp$ is the beam radius, and $U_0 = (1/\tau_0)\sqrt{K_{2r}/W_r}$ is the typical Rabi frequency of the probe field, with K_{2r} and W_r denoting the real parts of K_2 and W, respectively. Dimensionless coefficients are defined by $d_0 = L_D/L_A$ and $d_1 = L_D/L_{\rm diff}$, with $L_A = 1/(2\alpha)$ being the characteristic absorption length and $L_{\rm diff} = \omega_p R_\perp^2/c$ the characteristic diffraction length. In obtaining Eq. (26) we have assumed $L_D = L_{\rm NL}$, i.e., a balance of dispersion and nonlinearity, in order to favor the formation of solitons. If the conditions $d_0 \ll 1$ and $d_1 \ll 1$ are satisfied, Eq. (26) can be reduced to a standard nonlinear Schrödinger (NLS) equation, which is completely integrable and allows multisoliton solutions. A single bright soliton solution reads

$$u = 2\beta\,\mathrm{sech}\,[2\beta(\sigma - \sigma_0 + 4\delta s)] \times \exp[-2i\delta\sigma - 4i(\delta^2 - \beta^2)s - i\phi_0], \tag{27}$$

where β, δ, σ_0, and ϕ_0 are real free parameters that determine the amplitude (as well as the width), propagating velocity, initial position, and initial phase of the soliton, respectively. When taking $\beta = 1/2$ and $\delta = \sigma_0 = \phi_0 = 0$, we have $u = \mathrm{sech}\sigma\,\exp(is)$, or in terms of the field

$$\Omega_p = \frac{1}{\tau_0}\sqrt{\frac{K_{2r}}{W_r}}\,\mathrm{sech}\left[\frac{1}{\tau_0}\left(t - \frac{z}{\tilde{v}_g}\right)\right]\exp\left(iK_{0r}z + i\frac{z}{2L_D}\right), \tag{28}$$

which describes a bright soliton traveling with propagating velocity $\tilde{v}_g = \mathrm{Re}(v_g)$ and $K_{0r} = \mathrm{Re}[K(0)]$.

We now give a practical example for the formation of the optical soliton given above. We choose the ^{87}Rb D_1 line transition, with system parameters given by $\kappa_{13} = 5.0 \times 10^9\ \mathrm{cm^{-1}\ s^{-1}}$, $\Omega_c = 3.6 \times 10^7\ \mathrm{s^{-1}}$, $\Delta_2 = \Delta_3 = 3.5 \times 10^4\ \mathrm{s^{-1}}$, and $2\Delta\omega_D = 100\gamma_{31}$. With these parameters, we have $|\Omega_c|^2\gamma_{31}/(2\gamma_{21}\Delta\omega_D) = 8 \gg 1$, and hence the system is in the EIT regime. In this case, the coefficients in Eq. (25) are $K_2 = (1.4 + 0.3i) \times 10^{-12}\ \mathrm{cm^{-1}\ s^2}$ and $W = (2.0 + 0.04i) \times 10^{-15}\ \mathrm{cm^{-1}\ s^2}$. We see that the imaginary parts of these coefficients are indeed much smaller than their corresponding real parts. The physical reason for this small imaginary part is the quantum interference effect induced by the control field, by which the role of population and coherence decay rates for the propagation of the soliton is largely suppressed. When taking $\tau_0 = 1.5 \times 10^{-6}$ s and $R_\perp = 0.05$ cm, we have the characteristic lengths $L_D = 1.6$ cm, $L_A = 54.6$ cm, and $L_{\rm diff} = 200$ cm, which ensure the validity of neglecting absorption and diffraction of the probe pulse when the propagation distance is not much larger than the dispersion length, i.e., $d_0 \ll 1$ and $d_1 \ll 1$ are satisfied. We have to mention that the perturbation term $id_0 u$ in Eq. (26), contributed by population and coherence decay rates, may result in a small deformation of the soliton by decreasing its amplitude, increasing its width, and radiating small continuous dispersive waves (for a detailed discussion, see Ref. [30]), which is, however, not fatal for a soliton propagating to distance L_D. Using the above data it is easy to estimate the propagating velocity of the soliton, which reads

$$\tilde{v}_g = 6.6 \times 10^{-6} c. \tag{29}$$

Consequently, the optical soliton obtained may travel with an ultraslow propagating velocity in the Doppler-broadened EIT system.

The input power for generating the ultraslow optical soliton can be estimated by calculating Poynting's vector. The average flux of energy over a carrier-wave period is $\bar{P} = \bar{P}_{\max}\mathrm{sech}^2[(t - z/\tilde{v}_g)/\tau_0]$, with the peak power $\bar{P}_{\max} = 2\epsilon_0 c n_p S_0(\hbar/p_{13})^2 K_{2r}/(W_r\tau_0^2)$. Here, $n_p = 1 + cK_{0r}/\omega_p$ is the refractive index and S_0 is the cross-section area of the probe field. Using the above parameters, we obtain

$$\bar{P}_{\max} = 9.7 \times 10^{-6}\ \mathrm{W}. \tag{30}$$

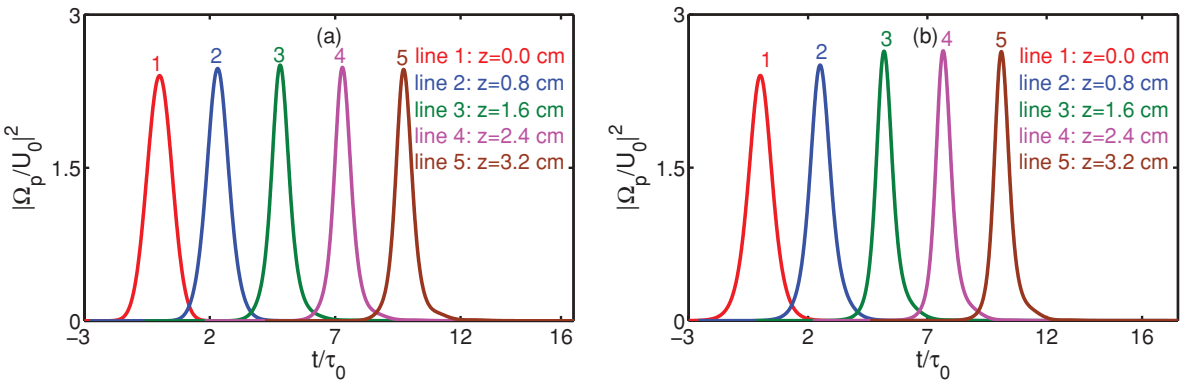

FIG. 5. (Color online) Evolution of dimensionless probe-field intensity $|\Omega_p/U_0|^2$ as a function of dimensionless time t/τ_0. Initial conditions are $\Omega_p(0,t)/U_0 = 1.6\ \exp(-t^2/\tau_0^2)$ (a) and $\Omega_p(0,t)/U_0 = 1.6\ \mathrm{sech}(1.6t/\tau_0)$ (b), respectively. In both panels, curves from 1 to 5 are wave shapes after propagating $z = 0.8$ cm, $z = 1.6$ cm, $z = 2.4$ cm, and $z = 3.2$ cm, respectively.

This is a drastic contrast to the case in conventional media such as optical fibers, where pico- or femtosecond laser pulses are usually needed to reach a very high peak power to stimulate enough nonlinearity for the formation of solitons.

To make a further confirmation of the soliton solutions and check their stability, we have made a numerical simulation directly from Eqs. (2a)–(2f) and (6). Shown in Fig. 5(a) is the result for $|\Omega_p/U_0|^2$ as a function of t/τ_0. The curves from 1 to 5 are wave shapes after propagating $z = 0.8$ cm, $z = 1.6$ cm, $z = 2.4$ cm, and $z = 3.2$ cm, respectively. The initial condition is given by a Gaussian form $u = 1.6\ \exp(-t^2/\tau_0^2)$. We see that when propagating to $z = L_D = 1.6$ cm the probe pulse becomes higher and sharper due to the self-phase-modulation induced by the Kerr effect. Then it suffers no serious distortion during the propagation, indicating the formation of an optical soliton in the system. Shown in Fig. 5(b) is the formation and propagation of an optical soliton with the initial condition being $u = 1.55\ \mathrm{sech}\,(1.55t/\tau_0)$.

An extra simulation for a stronger initial probe field has also been made, with the result shown in Fig. 6. We see that in this situation the wave shape of the probe pulse is well preserved within the distance L_D; however, as the propagation distance increases, a distortion of the pulse contributed by higher-order dispersion and high-order nonlinearity appears, which results in a raising of the pulse amplitude and a radiating of dispersive waves. We mention here that the regime when both probe and control fields are strong and both beams propagate together [62–66] is a topic of great interest, which is, however, beyond the scope of our present work.

The properties of collisions between two ultraslow optical solitons have also been investigated. We take $u = 1.0\ \mathrm{sech}(t/\tau_0)\exp(i\theta_1) + 1.0\ \mathrm{sech}(t/\tau_0 - 7.5)\exp(i\theta_2)$ as the initial condition, where θ_j $(j = 1,2)$ is the initial phase of the jth soliton. The result for $\Delta\theta = \theta_2 - \theta_1 = 0$ is shown in Fig. 7(a). We see that both solitons resume their original shapes after the collision and the interaction between them is repulsive. The physical essence of the repulsion phenomenon is that the light intensity in the central collision region is decreased by the overlap of the two solitons, which leads to a decrease of the refractive index, and hence more light is ejected from the central region. In addition, a phase shift is observed after the collision. In Fig. 7(b) we show the result for $\Delta\theta = \pi/2$, and a pair of attractive solitons is found. This phenomenon results in an increase in the light intensity in the central collision region because of the overlap of the two solitons, which leads to an increase of the refractive index and hence attracts more light to the central region.

IV. WEAK-LIGHT SPATIAL SOLITONS

In this section, we focus on the adiabatic regime in which the envelope of the probe pulse varies slowly with respect to time (i.e., the pulse duration τ_0 is large), so that the atomic response can follow the variation of the probe field adiabatically. In this regime the time-derivative terms (and hence the dispersion effect) in the MB Eqs. (2a)–(2f) and (6) can be safely neglected. We consider the possibility of the existence of spatial optical solitons in the system. The physical mechanism of realizing spatial solitons is the interplay and balance between diffraction and nonlinearity. In the case of $(1+1)$ dimensions- [67], a spatial soliton can form by use of cubic nonlinearity. The cubic nonlinearity can be obtained by Taylor-expanding the probe-field susceptibility with respect to the probe-field intensity. When only the leading order (third-order) nonlinearity is kept, the system supports the existence of stable $(1+1)$D spatial solitons; this has been shown in cold atomic systems under EIT

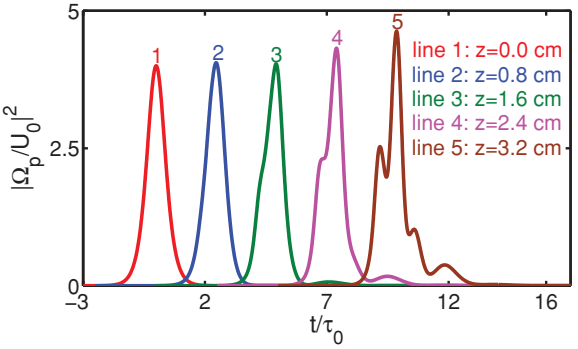

FIG. 6. (Color online) Evolution of stronger probe-field intensity $|\Omega_p/U_0|^2$ as a function of dimensionless time t/τ_0. Initial condition is $\Omega_p(0,t)/U_0 = 2.0\ \mathrm{sech}(2.0t/\tau_0)$. Curves from 1 to 5 are wave shapes after propagating $z = 0.8$ cm, $z = 1.6$ cm, $z = 2.4$ cm, and $z = 3.2$ cm, respectively.

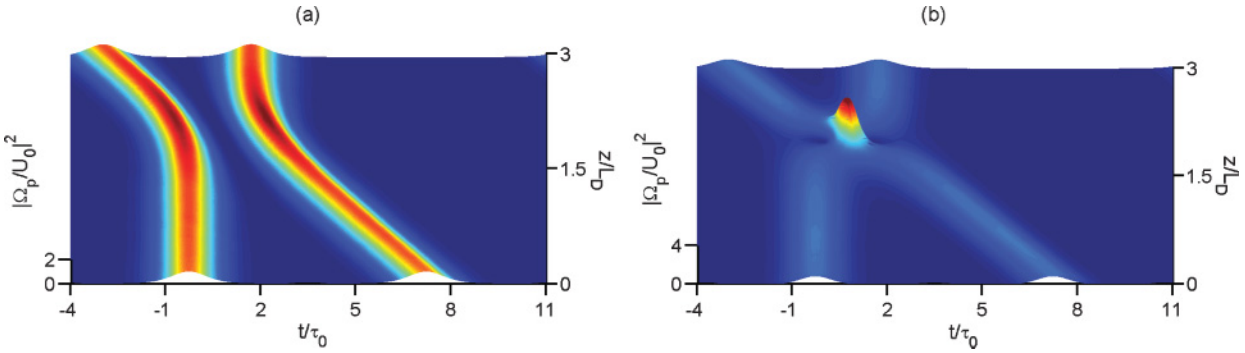

FIG. 7. (Color online) Wave shape of $|\Omega_p/U_0|^2$ with the initial condition given by $u = 1.0\ \mathrm{sech}(t/\tau_0)\exp(i\theta_1) + 1.0\ \mathrm{sech}\,(t/\tau_0 - 7.5)\exp(i\theta_2)$. (a) and (b) show collisions for $\Delta\theta \equiv \theta_2 - \theta_1 = 0$ and $\pi/2$, respectively. Parameters are given in the text.

conditions [68]. However, the existence of $(2+1)$D spatial solitons requires higher-order nonlinearities, and hence large probe field intensity, as shown in Refs. [31,69].

For a weak probe field with transverse radii $R_x \ll R_y$, only the diffraction in the x direction is significant. In this case the Maxwell Eq. (6) can be reduced to the form

$$i\frac{\partial}{\partial z}\Omega_p + \frac{c}{2\omega_p}\frac{\partial^2}{\partial x^2}\Omega_p + K_s\Omega_p - W_s|\Omega_p|^2\Omega_p = 0, \qquad (31)$$

where $K_s = k_p\chi_p^{(1)}/2$ and $W_s = -\kappa_{13}\varepsilon_0\hbar^3\chi_{pp}^{(3)}/(\mathcal{N}_a|\mathbf{p}_{13}|^4)$, $\chi_{pp}^{(3)}$ being given in Eq. (15b). Under the EIT condition, the imaginary parts of K_s and W_s are much smaller than their real parts. Neglecting the small imaginary part and taking the transformation $\Omega_p = F(z,x)\exp(iK_{sr}z)$, Eq. (31) can be recast into

$$i\frac{\partial}{\partial z}F + \frac{c}{2\omega_p}\frac{\partial^2}{\partial x^2}F - W_{sr}|F|^2F = 0. \qquad (32)$$

This is the $(1+1)$D NLS equation and allows single- and multisoliton solutions, which are well known in soliton theory and hence not presented here to save space.

However, if only the cubic nonlinearity is included, $(1+1)$D solitons are unstable for long-wavelength transverse perturbations. To realize a stable high-dimensional spatial optical soliton, higher-order nonlinearities must be included and thus the probe-field intensity must be strong enough. In the case of saturation nonlinearity, the Maxwell Eq. (6) takes the form

$$i\frac{\partial}{\partial z}\Omega_p + \frac{c}{2\omega_p}\left(\frac{\partial^2}{\partial x^2} + \frac{\partial^2}{\partial y^2}\right)\Omega_p + \kappa_{13}\int_v dv f(v)\frac{d_{21}\Omega_p}{D(1+V|\Omega_p|^2)} = 0, \qquad (33)$$

with $D = |\Omega_c|^2 - d_{21}d_{31}$ and $V = (|d_{21}|^2 + |\Omega_c|^2)/|D|^2$. Generally, it is very difficult to make an analysis of (33). For simplicity, we evaluate the integral in the last term of the RHS by replacing d_{31} with $\Delta_{31} + i\Delta\omega_D$, as all parameters are much smaller than the Doppler width. Then Eq. (33) is reduced to

$$i\frac{\partial}{\partial z}\Omega_p + \frac{c}{2\omega_p}\left(\frac{\partial^2}{\partial x^2} + \frac{\partial^2}{\partial y^2}\right)\Omega_p + \kappa_{13}\frac{d_{21}}{\tilde{D}(1+\tilde{V}|\Omega_p|^2)}\Omega_p = 0, \qquad (34)$$

where $\tilde{D} = (|\Omega_c|^2 + \gamma_{21}\Delta\omega_D - \Delta_3^2) - i\Delta_3\Delta\omega_D$ and $\tilde{V} = (\Delta_3^2 + |\Omega_c|^2)/[(|\Omega_c|^2 + \gamma_{21}\Delta\omega_D - \Delta_3^2)^2 + \Delta_3^2\Delta\omega_D^2]$. In obtaining Eq. (34), the condition of the control field being resonant has been assumed.

For a clear demonstration, we introduce dimensionless variables $s = z/L_{\mathrm{diff}}$, $(\xi,\eta) = (x,y)/R_\perp$, and $u = \Omega_p/U_0$, where $L_{\mathrm{diff}} = \omega_p R_\perp^2/c$, $R_\perp$, and $U_0 = 1/\sqrt{\tilde{V}}$ are the characteristic diffraction length, beam radius, and Rabi frequency of the probe field, respectively. With these variables, Eq. (34) can be written as the dimensionless form

$$i\frac{\partial u}{\partial s} + \frac{1}{2}\left(\frac{\partial^2}{\partial\xi^2} + \frac{\partial^2}{\partial\eta^2}\right)u + \frac{au}{1+|u|^2} = 0, \qquad (35)$$

where $a = \kappa_{13}d_{21}L_{\mathrm{diff}}/\tilde{D} \equiv a_r + ia_i$, with $a_r = \kappa_{13}L_{\mathrm{diff}}\Delta_3(|\Omega_c|^2 + \gamma_{21}\Delta\omega_D - \Delta_3^2)/[(|\Omega_c|^2 + \gamma_{21}\Delta\omega_D - \Delta_3^2)^2 + \Delta_3^2\Delta\omega_D^2]$ and $a_i = \kappa_{13}L_{\mathrm{diff}}\Delta_3^2\Delta\omega_D^2/[(|\Omega_c|^2 + \gamma_{21}\Delta\omega_D - \Delta_3^2)^2 + \Delta_3^2\Delta\omega_D^2]$. One recognizes that $a_i \propto \Delta_3^2$ when $|\Omega_c|^2 + \gamma_{21}\Delta\omega_D - \Delta_3^2 \neq 0$, and thus a_i can be greatly suppressed if Δ_3 is sufficiently small.

Because under the EIT condition one can obtain a practical set of system parameters that make $a_i \ll a_r$ (see below), in leading order approximation the coefficients of Eq. (35) can be taken as real. By introducing the transformation $u = \upsilon\exp(ia_r s)$ and assuming that the solution is cylindrically symmetric with the form $\upsilon(s,r = \sqrt{\xi^2+\eta^2}) = \exp(i\beta s)\psi(r)$, where β is a real wave number and $\psi(r)$ is a real function, Eq. (35) is reduced to

$$\frac{\partial^2\psi}{\partial r^2} + \frac{1}{r}\frac{\partial\psi}{\partial r} - 2\psi\left(\frac{a_r\psi^2}{1+\psi^2} + \beta\right) = 0. \qquad (36)$$

The propagation constant β can be determined by choice of the peak soliton amplitude $\psi(s=0) = \psi_0$. The boundary conditions for solving Eq. (36) are $\partial\psi/\partial r = 0$ at $r = 0$ and $\partial\psi/\partial r = \psi = 0$ at $r \to \infty$. We numerically integrate Eq. (36) by changing the value of β until the computed spatial profile $\psi(r)$ satisfies the given boundary conditions. The calculated result for several soliton profiles for different peak values $\psi(0)$ is shown in Fig. 8(a).From the figure we see that the soliton beam size varies inversely with its field amplitude.

The stability of $(2+1)$D spatial solitons has been investigated by use of the Vakhitov-Kolokolov (VK) criterion [70]. Shown in Fig. 8(b) is the power $P = 2\pi\int_0^\infty\psi(r)^2 r dr$ contained in each soliton versus the propagation constant β. We see that at each point of the curve we have $\partial P/\partial\beta > 0$.

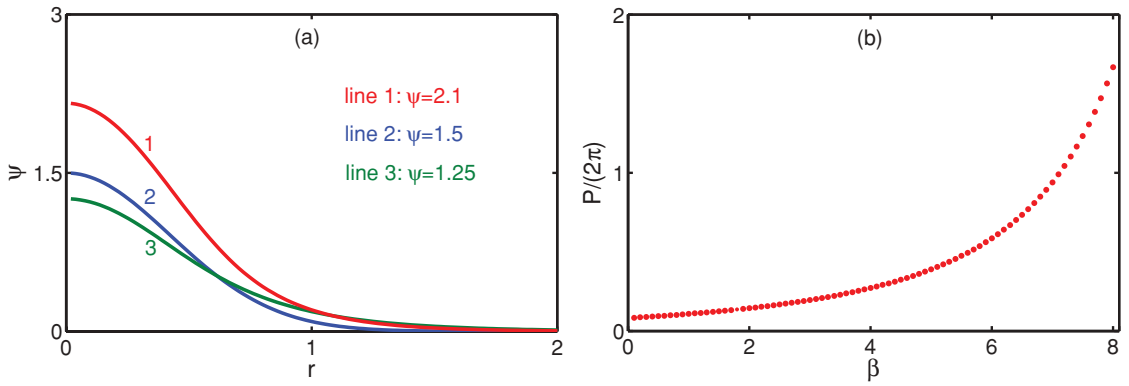

FIG. 8. (Color online) (a) Soliton profile ψ as a function of radial coordinate r, obtained by numerically integrating Eq. (36) with $a_R = -15.4$. Profiles labeled 1, 2, and 3 are for the peak value ψ_0 of 2.1, 1.5, and 1.25, respectively. (b) The power P of each soliton versus propagation constant β.

According to the VK criterion, this proves that the $(2+1)$D spatial optical soliton obtained is stable.

We use the ^{87}Rb D_1 line transition as a practical example for obtaining the $(2+1)$D spatial soliton in the system with Doppler broadening. Parameters are taken as $\kappa_{13} = 2.5 \times 10^{11}$ cm^{-1} s^{-1}, $\Omega_c = 3.6 \times 10^7$ s^{-1}, $\gamma_{21} = 10^{-4}\gamma_{31}$, $2\Delta\omega_D = 100\gamma_{31}$, $\Delta_3 = -0.4 \times 10^5$ s^{-1}, and $R_x = 50$ μm. With these parameters we obtain the characteristic diffraction length $L_{\text{diff}} = 2.0$ cm and $a = -15.4 + 1.0i$. Thus the imaginary part of a is about 15 times smaller than the real part and hence can be neglected safely. Although the Vakhitov-Kolokolov criterion holds only for a conservative limit, we expect that a very small dissipative perturbation will induce only a small deformation of the spatial soliton.

We have also made a numerical simulation for Eq. (35) by using a split-step Fourier method. Figure 9 shows the results of probe-field intensity $|\Omega_p/U_0|^2$ versus s. In the simulation a Gaussian initial condition $u = 0.7\exp[-(\xi^2+\eta^2)]$ is taken, which is shown in Fig. 9(a) with the beam's center located at the origin of the x-y plane. Plotted in Fig. 9(b) is the resulting probe beam at propagation distance $s = 2.5$, which shows indeed that the initial Gaussian beam shown in Fig. 9(a) evolves into a $(2+1)$D spatial soliton as s increases.

V. DISCUSSION AND SUMMARY

In this work, we have presented a systematic theoretical study for dealing with linear and nonlinear light propagations in a Doppler-broadened three-level Λ system. In our model, both the decoherence contributed by the incoherent population exchange between two lower energy levels and the decoherence due to the dephasing of off-diagonal elements of the density matrix have been taken into account. Through a careful analysis of the base state and the linear excitation of the system, we have illustrated clearly the relative importance of these two decoherence mechanisms. We have shown that, if $|\Omega_c|^2\gamma_{31} \ll 2\gamma_{21}\Delta\omega_D^2$, the incoherent population exchange is significant. Although in this situation a small dip may appear in the absorption profile of the probe field, it is not an EIT because the appearance of this small dip is due to the gain contributed by the incoherent population exchange. However, under the condition $|\Omega_c|^2\gamma_{31} \gg 2\gamma_{21}\Delta\omega_D^2$ the dephasing becomes the main source of decoherence. In this case, the incoherent population exchange effect is negligible and hence the system supports an EIT. The argument in the literature about the EIT criterion in Doppler-broadened media is thus clarified. The EIT criterion (9) also ensures the validity of the weak nonlinear perturbation theory used in this work for solving the MB equations with inhomogeneous broadening. Another important aspect of this work is the study of nonlinear excitations and their stable propagation in the system. We have shown that it is indeed possible to form temporal optical solitons in a Doppler-broadened medium. Such solitons have ultraslow propagating velocity and can be generated in very low light power. In addition, we have also demonstrated the possibility of realizing $(1+1)$D and $(2+1)$D spatial optical solitons in the adiabatic regime of this Doppler-broadened system. Note that in many systems, such as atomic and

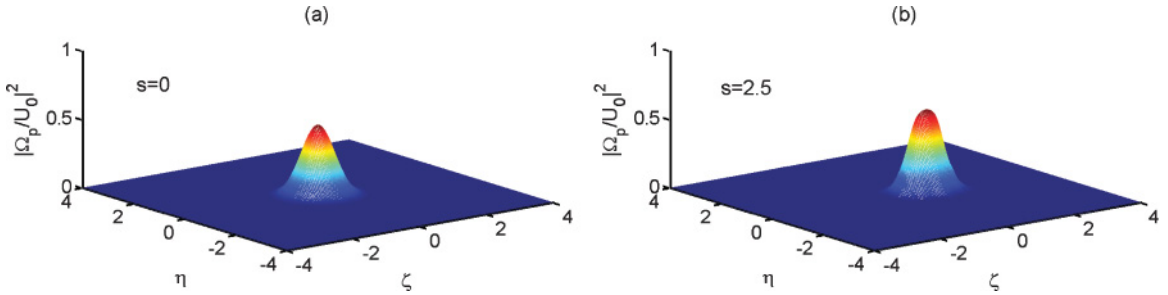

FIG. 9. (Color online) Formation and propagation of $(2+1)$D spatial optical solitons. (a) The initial Gaussian beam. (b) Formation of $(2+1)$D spatial optical soliton by the evolution of the Gaussian beam at distance $s = 2.5$.

molecular gases filled in hollow-core photonic-crystal band-gap fibers, both dephasing and incoherent population exchange play significant roles [71]. The theoretical method proposed in the present work can be applied to such systems with inhomogeneous broadening. The results predicted here may be useful for guiding experimental investigations of linear and nonlinear optical properties of inhomogeneously broadened systems and for applications of optical information processing and engineering based on hot vapors.

ACKNOWLEDGMENTS

G.H. thanks M. Xiao for many fruitful discussions. This work was supported by NSF-China under Grants No. 10434060 and No. 10874043 and by the Key Development Program for Basic Research of China under Grants No. 2005CB724508 and No. 2006CB921104.

APPENDIX: EXPLICIT EXPRESSIONS OF $\mathcal{K}_1$ AND $\mathcal{K}_2$

For the pole at $k_p v = -i\Delta\omega_D$, we obtain

$$\mathcal{K}_1 = -\frac{i\sqrt{\pi}\kappa_{13}}{2AZ_1}[(B_1-\omega^2)+i\Delta\omega_D\omega](C_1+iD_1\omega), \tag{A1}$$

where

$$A = -2\gamma_{21}\Delta\omega_D^2 + \gamma_{31}|\Omega_c|^2, \tag{A2a}$$

$$Z_1 = \Delta\omega_D^2\omega^2 + (|\Omega_c|^2 + \gamma_{21}\Delta\omega_D - \omega^2)^2, \tag{A2b}$$

$$B_1 = |\Omega_c|^2 + \gamma_{21}\Delta\omega_D, \tag{A2c}$$

$$C_1 = -2\gamma_{21}\gamma_{31}|\Omega_c|^2 + 2\gamma_{21}(2\gamma_{21}-\Gamma_{21})\Delta\omega_D^2 + 2\gamma_{21}\Gamma_{21}|\Omega_c|^2\Delta\omega_D, \tag{A2d}$$

$$D_1 = -2(2\gamma_{21}-\Gamma_{21})\Delta\omega_D^2 + 2\gamma_{31}|\Omega_c|^2. \tag{A2e}$$

For the pole at $k_p v = -i\sqrt{\gamma_{31}|\Omega_c|^2}/(2\gamma_{21})$, we obtain

$$\mathcal{K}_2 = \frac{i\sqrt{\pi}\kappa_{13}\Gamma_{21}\gamma_{31}|\Omega_c|^2\Delta\omega_D}{2\gamma_{21}AZ_2 y}[(B_2-\omega^2)+iy\omega](C_2+i\omega), \tag{A3}$$

where $y = \sqrt{\gamma_{31}|\Omega_c|^2/(2\gamma_{21})}$ and

$$Z_2 = (|\Omega_c|^2 + \gamma_{21}y - \omega^2)^2 + y^2\omega^2, \tag{A4a}$$

$$B_2 = |\Omega_c|^2 + \gamma_{21}y, \tag{A4b}$$

$$C_2 = -\gamma_{21} + \frac{|\Omega_c|^2}{y}. \tag{A4c}$$

When obtaining the expressions for$\mathcal{K}_1$ and $\mathcal{K}_2$, we have assumed the condition (8) and $\Delta\omega_D \gg |\Omega_c|, \gamma_{31} \gg \gamma_{21}, \Gamma_{21}$, i.e., all parameters are assumed much smaller than the Doppler width.

[1] S. E. Harris, Phys. Today **50**, 36 (1997).
[2] M. Fleischhauer, A. Imamoglu, and J. P. Marangos, Rev. Mod. Phys. **77**, 633 (2005).
[3] K. Hammerer, A. S. Sorensen, and E. S. Polzik, Rev. Mod. Phys. **82**, 1041 (2010).
[4] S. E. Harris, J. E. Field, and A. Imamoglu, Phys. Rev. Lett. **64**, 1107 (1990).
[5] H. Schmidt and A. Imamoglu, Opt. Lett. **21**, 1936 (1996).
[6] M. D. Lukin, P. R. Hemmer, M. Löffler, and M. O. Scully, Phys. Rev. Lett. **81**, 2675 (1998).
[7] S. E. Harris and L. V. Hau, Phys. Rev. Lett. **82**, 4611 (1999).
[8] H. Wang, D. Goorskey, and M. Xiao, Phys. Rev. Lett. **87**, 073601 (2001).
[9] H. Kang and Y. Zhu, Phys. Rev. Lett. **91**, 093601 (2003).
[10] Z.-B. Wang, K.-P. Marzlin, and B. C. Sanders, Phys. Rev. Lett. **97**, 063901 (2006).
[11] C. Hang, Y. Li, L. Ma, and G. Huang, Phys. Rev. A **74**, 012319 (2006).
[12] H. Sun, S. Gong, Y. Niu, Shiqi Jin, Ruxin Li, and Zhizhan Xu, Phys. Rev. B **74**, 155314 (2006).
[13] M. V. Pack, R. M. Camacho, and J. C. Howell, Phys. Rev. A **74**, 013812 (2006).
[14] M. V. Pack, R. M. Camacho, and J. C. Howell, Phys. Rev. A **76**, 033835 (2007).
[15] D. D. Yavuz and D. E. Sikes, Phys. Rev. A **81**, 035804 (2010).
[16] J. C. Petch, C. H. Keitel, P. L. Knight, and J. P. Marangos, Phys. Rev. A **53**, 543 (1996).
[17] Y. Li and M. Xiao, Opt. Lett. **21**, 1064 (1996).
[18] M. M. Kash, V. A. Sautenkov, A. S. Zibrov, L. Hollberg, G. R. Welch, M. D. Lukin, Y. Rostovtsev, E. S. Fry, and M. O. Scully, Phys. Rev. Lett. **82**, 5229 (1999).
[19] L. Deng, M. Kozuma, E. W. Hagley, and M. G. Payne, Phys. Rev. Lett. **88**, 143902 (2002).
[20] Y. Wu, J. Saldana, and Y. F. Zhu, Phys. Rev. A **67**, 013811 (2003).
[21] L. Deng and M. G. Payne, Phys. Rev. Lett. **91**, 243902 (2003).
[22] D. A. Braje, V. Balic, S. Goda, G. Y. Yin, and S. E. Harris, Phys. Rev. Lett. **93**, 183601 (2004).
[23] H. Kang, G. Hernandez, and Y. F. Zhu, Phys. Rev. Lett. **93**, 073601 (2004).
[24] Y. P. Niu, R. Li, and S. Gong, Phys. Rev. A **71**, 043819 (2005).
[25] Z. C. Zuo, J. Sun, X. Liu, Q. Jiang, G. S. Fu, L. A. Wu, and P. M. Fu, Phys. Rev. Lett. **97**, 193904 (2006).
[26] Y. P. Zhang, A. W. Brown, and M. Xiao, Phys. Rev. Lett. **99**, 123603 (2007).
[27] V. Boyer, C. F. McCormick, E. Arimondo, and P. D. Lett, Phys. Rev. Lett. **99**, 143601 (2007).
[28] Y. P. Zhang, U. Khadka, B. Anderson, and M. Xiao, Phys. Rev. Lett. **102**, 013601 (2009).
[29] Y. Wu and L. Deng, Phys. Rev. Lett. **93**, 143904 (2004).
[30] G. Huang, L. Deng, and M. G. Payne, Phys. Rev. E **72**, 016617 (2005).
[31] H. Michinel, M. J. Paz-Alonso, and V. M. Perez-Garcia, Phys. Rev. Lett. **96**, 023903 (2006).
[32] C. Hang, G. Huang, and L. Deng, Phys. Rev. E **73**, 036607 (2006).
[33] Y. Wu and X. Yang, Appl. Phys. Lett. **91**, 094104 (2007).
[34] C. Hang and G. Huang, Phys. Rev. A **77**, 033830 (2008).

[35] L.-G. Si, W.-X. Yang, and X. Yang, J. Opt. Soc. Am. B **26**, 478 (2009).
[36] C. Hang, V. V. Konotop, and G. Huang, Phys. Rev. A **79**, 033826 (2009).
[37] W.-X. Yang, A.-X. Chen, L.-G. Si, K. Jiang, X. Yang, and R.-K. Lee, Phys. Rev. A **81**, 023814 (2010).
[38] J. Gea-Banacloche, Y. Q. Li, S. Z. Jin, and M. Xiao, Phys. Rev. A **51**, 576 (1995).
[39] A. Javan, O. Kocharovskaya, H. Lee, and M. O. Scully, Phys. Rev. A **66**, 013805 (2002).
[40] C. Y. Ye and A. S. Zibrov, Phys. Rev. A **65**, 023806 (2002).
[41] H. Lee, Y. Rostovtsev, C. J. Bednar, and A. Javan, Appl. Phys. B **76**, 33-39 (2003).
[42] U. D. Rapol, A. Wasan, and V. Natarajan, Phys. Rev. A **67**, 053802 (2003).
[43] Y. Rostovtsev, I. Protsenko, H. Lee, and A. Javan, J. Mod. Opt. **49**, 2501 (2002).
[44] P. R. S. Carvalho, L. E. E. de Araujo, and J. W. R. Tabosa, Phys. Rev. A **70**, 063818 (2004).
[45] C. Goren, A. D. Wilson-Gordon, M. Rosenbluh, and H. Friedmann, Phys. Rev. A **69**, 063802 (2004).
[46] A. J. Krmpot, M. M. Mijailovic, B. M. Panic, D. V. Lukic, A. G. Kovacevic, D. V. Pantelic, and B. M. Jelenkovic, Opt. Express **13**, 1448 (2005).
[47] M. V. Pack, R. M. Camacho, and J. C. Howell, Phys. Rev. A **76**, 013801 (2007).
[48] S. M. Iftiquar and V. Natarajan, Phys. Rev. A **79**, 013808 (2009).
[49] O. Firstenberg, M. Shuker, R. Pugatch, D. R. Fredkin, N. Davidson, and A. Ron, Phys. Rev. A **77**, 043830 (2008).
[50] M. A. Kumar and S. Singh, Phys. Rev. A **79**, 063821 (2009).
[51] O. Kocharovskaya, Y. Rostovtsev, and M. O. Scully, Phys. Rev. Lett. **86**, 628 (2001).
[52] S. Shepherd, D. J. Fulton, and M. H. Dunn, Phys. Rev. A **54**, 5394 (1996).
[53] G. Vemuri and G. S. Agarwal, Phys. Rev. A **53**, 1060 (1996).
[54] J. R. Boon, E. Zekou, D. McGloin, and M. H. Dunn, Phys. Rev. A **59**, 4675 (1999).
[55] N. Mulchan, D. G. Ducreay, R. Pina, M. Yan, and Y. Zhu, J. Opt. Soc. Am. B **17**, 820 (2000).
[56] A. V. Gorshkov, A. André, M. D. Lukin, and A. S. Sørensen, Phys. Rev. A **76**, 033806 (2007).
[57] O. Firstenberg, M. Shuker, N. Davidson, and A. Ron, Phys. Rev. Lett. **102**, 043601 (2009).
[58] E. Figueroa, F. Vewinger, J. Appel, and A. I. Lvovsky, Opt. Lett. **31**, 2625 (2006).
[59] In the literature, there are different definitions of the Doppler width $\Delta\omega_D$. In this work, we define $\Delta\omega_D = k_p v_T$.
[60] In the literature, it is also called the ground state of the MB equations (2) and (6). Here we use the name "base state" to avoid possible confusion with the atomic ground state $|1\rangle$.
[61] B. Luo, C. Hang, H.-J. Li, and G. Huang, Chin. Phys. B **19**, 054214 (2010).
[62] R. Grobe, F. T. Hioe, and J. H. Eberly, Phys. Rev. Lett. **73**, 3183 (1994).
[63] M. Fleischhauer, A. S. Manka, Phys. Rev. A **54**, 794 (1996).
[64] K. M. Paul, J. R. Csesznegi, and R. Grobe, Laser Phys. **7**, 884 (1997).
[65] J. R. Csesznegi and R. Grobe, Phys. Rev. Lett. **79**, 3162 (1997).
[66] B. D. Clader and J. H. Eberly, Phys. Rev. A **76**, 053812 (2007).
[67] Here, the first "1" refers to the transverse spatial coordinate, and the second "1" to the propagation coordinate z.
[68] T. Hong, Phys. Rev. Lett. **90**, 183901 (2003).
[69] C. Hang, G. Huang, and L. Deng, Phys. Rev. E **74**, 046601 (2006).
[70] M. G. Vakhitov and A. A. Kolokolov, Izv. Vyssh. Uchebn. Zaved., Radiofiz. **16**, 1020 (1973) [Sov. J. Radiophys. Quantum Electron. **16**, 783 (1973)].
[71] A. D. Slepkov, A. R. Bhagwat, V. Venkataraman, P. Londero, and A. L. Gaeta, Phys. Rev. A **81**, 053825 (2010).